

# **The Role of Hydroxyl Groups in the Self-Assembly of Long Chain Alkyl Hydroxyl Carboxylic Acids on Mica.**

**José J. Benítez<sup>1,\*</sup>, José A. Heredia-Guerrero<sup>1</sup>, Francisco M. Serrano<sup>1</sup> and Antonio Heredia<sup>2</sup>.**

<sup>1</sup> Instituto de Ciencia de Materiales de Sevilla, Centro Mixto CSIC-Universidad de Sevilla. Avda. Americo Vespuccio 49, 41092 Sevilla (Spain).

<sup>2</sup> Departamento de Biología Molecular y Bioquímica. Facultad de Ciencias. Universidad de Málaga, E-29071 Málaga (Spain).

\* To whom correspondence should be addressed.

Email: [benitez@icmse.csic.es](mailto:benitez@icmse.csic.es)

## **ABSTRACT**

The adsorption and self-assembly of hydroxylated long chain fatty acids on mica has been studied by AFM. The presence of secondary mid-chain hydroxyl groups is found to strongly affect the self-assembly process via the reinforcement of lateral interactions between molecules by -OH...HO- hydrogen bonding. On the other side, the availability of an exposed terminal hydroxyl group in the acid molecule triggers the formation of a second layer due to the strength of the -OH...HOOC- tail to head interaction.

Surface coverage ( $\theta$ ) data follows a Langmuir type relationship vs solution concentration ( $c$ ). The analysis of the slope of  $1/\theta$  vs  $1/c$  plots provides a relative estimation of the adsorption enthalpy for the formation of the first and second monolayers. Based on that, both the contribution of molecule-substrate and lateral

molecule-molecule energy terms are found to be relevant in the self-assembly of this type of molecules on mica.

## **INTRODUCTION**

Adsorption and packing of long chain fatty acids, as well as disubstituted alkanes (diols, dioic and hydroxy acids), on graphite have been extensively studied by STM<sup>1,2,3,4</sup>. Results clearly demonstrate that end group interactions between these molecules are dominated by hydrogen bonding. However, much less attention has been paid to the role of secondary hydroxyl groups in the interaction of long chain self-assembled alkyl molecules.

Our interest in such molecules is because long chain alkyl and alkyl hydroxylated fatty acids are the monomers units of several biopolymers such as cutin<sup>5,6</sup>. Cutin is the most abundant polyester in nature and constitutes the framework of the protective cuticle of stems and leaves of higher plants. Besides, synthetic cutins can be obtained in the laboratory from a mixture of 9(10), 16-dihydroxyhexadecanoic acid and a small amount of 16-hydroxyhexadecanoic acid monomers<sup>7</sup>, which opens a chemical route to an interesting non toxic and biodegradable biomimetic material.

Though the chemical composition of these biopolymers is well known, very little information about their intra-molecular structure and its formation in nature is still available<sup>8,9</sup>. Recently we have proposed molecular self-assembly, i.e. the creation of ordered three dimensional structures by individual incorporation of monomeric and/or supramolecular units through weak chemical forces, as an operative mechanism, at least in the early stages of formation of cutin in nature<sup>10</sup>.

We are using the molecular self-assembly approach as a model to investigate the interaction between primary and secondary hydroxyl groups in a geometrically well

defined environment as the one imposed by SAMs on mica<sup>11</sup>. For this purpose, we have selected three long chain alkyl molecules such as 9(10),16-dihydroxypalmitic, 12-hydroxystearic and palmitic acids as models containing one secondary/one primary, one secondary and no hydroxyl groups, respectively. By means of AFM, we study the role of such hydroxyl groups in defining a layer growing pattern on the surface of mica and how the conclusions can be extended to the understanding of the genesis and short range structure of biopolymer cutin<sup>12,13,14</sup>.

## **EXPERIMENTAL**

Palmitic acid (PA) (99%) and 12-hydroxystearic acid (HSA) (99%) were purchased from Aldrich and used without further purification. Formally, the use of a secondary hydroxylated palmitic acid (16 C atoms) molecule instead of HSA (18 C atoms) would be desirable, however this product cannot commercially be obtained. From previous results in the literature, we expect no significant differences in the self-assembly process caused by the presence of two extra carbon atoms in such long alkyl molecules.

9(10),16-dihydroxypalmitic acid (diHPA) is not a commercial product and had to be obtained by depolymerization of natural biopolyester cutin from cuticles of tomato fruits as described elsewhere<sup>11</sup>.

Solutions 0.1 - 15mM were prepared from successive dilution of a concentrated mother solution 15 mM always using chloroform as solvent. In the case of the diHPA acid, a small amount of ethanol (8% by volume) had to be added to complete solution at such concentration. Mica (Muscovite) pieces were doubly cleaved at room conditions using an adhesive tape and immersed in solutions for 30 to 60 seconds depending on the molecule studied. Longer immersion time (up to 5 minutes) has been checked to have

no significant influence on the surface coverage observed. Samples were dried in a N<sub>2</sub> stream for 2-3 minutes, stored inside a test tube and analyzed typically 24 hours later. Sample ripening was carried out inside a Petri dish at laboratory temperature and humidity conditions.

AFM used is a Topometrix Explorer operating in air (20-25 °C, 40-45 % RH) and equipped with a big range (130x130µm<sup>2</sup> X-Y) scanner. The microscope was operated in contact mode at nominal forces very close to the pull-off point to minimize damage. From contact curves obtained, the estimated total force exerted by the tip on the islands is about 3-5 nN. The AFM head is calibrated using a TGZ01 (22 nm step height) grid purchased from NT-MDT. The same silicon nitride sharpened “V-shaped” Park Microlever with k=0.05 N/m was used along the whole series of experiments. Image analysis was done either using the WSxM 4.0 program provided by Nanotec (Spain)<sup>15</sup> or the one built-in by Topometrix (Topometrix SPML v. 4.00). Reproducibility of AFM images were ensured by scanning large areas is at least 3 points of the surface and after two preparations. Surface coverage was obtained by several methods: (i) surface flooding, (ii) height histogram deconvolution and (iii) bearing ratio diagram. A very good correlation was found in every case following those three methods. Surface coverage values reported are the average of at least 20 measurements for each molecule and concentration studied. Standard deviations are 9%, 6% and 5% for PA, HSA and diHPA, respectively.

Height measurements are carried out directly from topographic line profiles. Typically 10-15 random, both trace and retrace, lines per image are analyzed. Standard deviation values observed are in the 5-6% with no relevant differences between trace and retrace measurements, which discards the coupling between the topographic and the frictional signals.

Height measurements from histograms in our samples have shown to systematically provide slightly lower values than line profiles. This is a software induced error of background subtraction in our images which overestimates background height and underestimates island values.

Attempts to resolve the structure of the islands at the molecular scale have been made. Unfortunately, and like in a similar system and experimental setup<sup>16</sup>, damage exerted by the scanning tip prevents to obtain molecular resolution AFM images. Consequently, our conclusions are based on large scale data.

AFM images are presented along the paper in different scales to allow a realistic visualization of topography.

## **RESULTS AND DISCUSSION.**

### **1. Palmitic acid (PA) self-assembly.**

AFM study of the adsorption and self assembly of palmitic acid on mica is shown in figure 1. The series is prepared from chloroform solutions with increasing concentrations of the alkyl molecule. The upper row displays the 20  $\mu\text{m}$  x 20  $\mu\text{m}$  AFM images obtained after 24 hours ripening at room conditions. The lower row is obtained from the same samples shown above after much longer ripening time at room conditions (10 to 15 days). The first observation is the wide range of island sizes showing no pattern with solution concentration. We interpret this result assuming that PA adsorption and self-assembly on mica is composed of two stages: (i) adsorption and (ii) molecular diffusion and packing. Our preparation method seems to have no control on the second stage, likely due to the variables affecting the transference of PA molecules from the solution to the support<sup>17,18</sup>. Consequently, sizes and shapes of islands changes from experiment to experiment. In most cases island are dendritic and contains many

tinny holes. Island height is typically 2.0 nm, in good agreement with the values reported elsewhere<sup>17,18,19,20,21</sup>, except for those prepared from low concentration solutions which are 1.5 nm (low ripening time) and 1.5-1.8 nm (longer ripening). Often, a tilted molecular packing is proposed to explain height values below the molecule length. Also, island compression caused by the pressure exerted by the tip while scanning in contact mode is feasible. Such compression is likely to be more severe on less compact islands as those expected from less concentrated solutions and after lower ripening time, as observed here.

Interestingly, and despite the increasing concentration of PA in solution, a relatively constant surface coverage (12 – 15 %) is systematically obtained after 24 hours ripening, i.e. there is no increasing dependence with palmitic acid concentration in the preparation solution. This is an indication of saturation of adsorption sites and the reaching of an equilibrium state in the first stage proposed, i.e. the adsorption of palmitic acid molecules on mica.

Particularly, at the higher concentration tried (15 mM) a higher coverage value is obtained ( $\approx 24\%$ ) in the same conditions. Though, out of the scope of this article, we can think about the formation of palmitic acid dimers, as adsorption unit per adsorption site, as an argument to explain such increment. Indeed, dimerization of palmitic acid molecules has been described at the air/aqueous interface in conditions in which  $-\text{COOH}$  dissociation is hindered<sup>22</sup>.

Ripening also leads to an increase in surface coverage, which is shown at the lower row of figure 1. The increment ratio is constant along the entire concentration series. We interpret this result as the completion of the second stage: the effective self assembly of scattered palmitic acid molecules left on the surface of mica after preparation. At low ripening time, PA molecules either are easily displaced by the tip

while scanning in contact mode or they form ensembles small enough to be out of the operation resolution limit of the AFM microscope. In any case, they cannot be detected until they do not aggregate sufficiently after longer ripening. The total surface coverage obtained after full aggregation of palmitic acid (weak acid) molecules is achieved is 25-30%. This value can be considered as the actual saturation limit and it is very close to the one obtained in analogous preparation conditions for similar alkyl amines (weak base) (30-35%)<sup>23</sup>. This observation supports the participation of residual water molecules (amphoterous) from atmosphere in the structure of adsorption sites on mica in acid-base reaction, as already proposed in that article. Dynamic diffusion, aggregation and clustering of water molecules on mica surface are likely to be responsible for islands development, either by the formation of new ones (as observed at 1.5 and 5 mM) or by increasing their size (3, 10 and 15 mM, in figure 1).

Despite the lack of pattern and such a variety of island topography, PA molecule self-assembly is a good reference to remark the differences introduced by the presence of primary and secondary hydroxyl groups in the alkyl chain.

## **2. 12- hydroxystearic acid (HSA) self-assembly.**

Adsorption and self-assembly of 12-hydroxystearic acid (HSA) on mica is quite different if compared to palmitic acid. AFM images, figure 2, reveal a much higher surface coverage under similar preparation conditions (upper row). Values close to 100% are quickly and easily achieved from relatively diluted solutions. Besides, surface coverage of HSA is both concentration and adsorption time dependent.

While saturation of adsorption sites on mica surface is proposed for palmitic acid, it obvious that there is another parameter influencing the self-assembly of mid-chain hydroxylated molecules. Thus, lateral interaction between hydroxylated alkyl

molecules (hydrogen bonding through secondary hydroxyl groups) is proposed as an additional factor reinforcing the cohesive energy of self-assembled islands. Molecular sticking to the support involves, both, mica adsorption sites and lateral hydroxyl anchoring points. Consequently, HSA adsorption will proceed beyond surface saturation found for palmitic acid because of the availability of additional sticking points. This argument explains the time and concentration dependence of HSA adsorption and self assembly. The limit for this model is the formation of a full monolayer, as observed experimentally.

The lateral interaction between hydroxyl groups is so fast and effective that there is no surface coverage dependence with ripening time, as observed for palmitic acid (figure 1) and other non hydroxylated long chain alkyl molecules<sup>23</sup>. Scattered molecules are quickly incorporated to self-assembled islands via hydrogen bonding between secondary hydroxyl groups.

HSA island height is typically 2.2 nm (line profile in figure 2), though values of 1.7-1.8 nm have been measured for low coverage samples. HSA molecule is longer than palmitic acid, the two extra carbon atoms in the molecule backbone add about 0.25 nm. Thus, despite the more extended aggregation and self assembly of HSA than palmitic acid, very similar height values are obtained. This means the same tilting angle of molecular packing and/or the same compressibility of both layers under the tip pressure. In the later case, the presence of steric hindrances caused by hydroxyl group can be expected to reduce the compactness of layers and may leading to a better compressibility. However, the reinforcement of lateral interaction caused by hydrogen bonding between these groups is acting in the opposite direction and both effects seem to compensate.



### 3. 9(10), 16 dihydroxypalmitic acid (diHPA) self-assembly.

Adsorption and packing of 9(10), 16 dihydroxypalmitic acid (diHPA) on mica has been studied in detail because our interest in this molecule as the main monomer of natural cutin, as mentioned in the introduction section.

Figure 3 shows the  $6 \times 6 \mu\text{m}^2$  topographic AFM images after adsorption of diHPA on mica from chloroform solutions. As observed, the support is progressively covered by the adsorbate to almost 100% at 10 mM.

A comparative surface coverage evolution vs solution concentration for the molecules studied is shown in figure 4. As it can be noted, HSA and diHPA (both containing secondary hydroxyl groups) are more effective than palmitic acid to reach a higher coverage. Besides, diHPA has an additional feature, it is capable of generating a second monolayer before completing the first one. Such a tendency has not been observed in molecules having no terminal (primary) hydroxyl group like palmitic and HSA.

The growing second monolayer can be seen as brighter areas in the images in figure 3. Thus, topographic profile obtained for the sample prepared at 10mM reveals a layer height of 5.5 nm with some spots at 2.5 nm. The monolayer height of diHPA (2.5 nm) is higher than the value of HSA (2.2 nm), despite the shorter alkyl chain backbone (16 vs 18 carbon atoms, respectively). This observation can be explained by the extra terminal to terminal hydroxyl groups interaction between diHPA molecules forcing the alkyl chains to pack fully vertical <sup>11</sup>.

The process of the second monolayer development can be seen in detail in figure 5 by plotting height histograms along the concentration series. The evolution of both the total surface coverage and the growth of the second monolayer are also included in the figure at the bottom-right corner.

Coverage data ( $\theta$ ) vs solution concentration ( $c$ ) for HSA and diHPA, figures 4 and 5, can be fitted to a Langmuir type isotherm ( $\theta = bc/(1+bc)$ ). Plots are shown in figure 6 and the slope of linear fittings is  $1/b$ . In a Langmuir isotherm ( $b$ ) is defined as the ratio between rate constants for adsorption ( $k_a$ ) and desorption ( $k_d$ ) processes. In figure 6, two sets of data can be observed (open and shaded symbols, respectively). Both the adsorption of HSA and the first monolayer of diHPA (shaded symbols) show a very similar  $b$  value, while the formation of the second layer of diHPA (open triangles) has a lower  $b$ .

Among others parameters, the constant ( $b$ ) is a function of the enthalpy of adsorption. To extract enthalpy values, isotherms at several temperature values should be obtained. Our results are obtained only at RT, consequently, the following discussion is qualitative, and assumes that the variation of enthalpy is the major contribution to the modification of the slope of the isotherms. The energy involved in the process of adsorption and packing of HSA and diHPA molecules into a monolayer on mica, can be expressed as the contribution of both a molecule to substrate and a molecule to molecule terms. The interaction of HSA and diHPA molecules with mica is via the carboxylic group, besides the molecule to molecule cohesive energy, in both cases, it is also ruled by the hydrogen bonding between secondary hydroxyl groups. Thus, it is reasonable to justify the similarity of ( $b$ ) values by the assumption of the same interactions involved.

However, the formation of the second monolayer of diHPA necessarily means the adsorption of the molecule on top of a pre-existing one. Though the structure of the bilayer cannot be precisely stated from our experimental results, previous results on the adsorption of long chain alkyl alcohols and hydroxyl acids on mica<sup>11</sup>, make reasonable to consider that the diHPA molecule is adsorbed on mica through the carboxyl group

leaving the terminal hydroxyl group as the anchoring point for the second layer. The interaction between carboxyl and hydroxyl groups has been defined to be in the order  $\text{COOH}\dots\text{HOOC} > \text{-COOH}\dots\text{HO} > \text{-OH}\dots\text{HO}^{-4}$ , so it is reasonable to postulate that the second layer is formed by the interaction of the carboxyl group of the adsorbing molecule with the terminal hydroxyl group of the pre-adsorbed one. Lateral interactions between hydroxyl groups of diHPA molecules are also operative in the second layer, so their contribution to the overall energy is expected to be same as in the first layer. However, the molecule to substrate interaction has changed for the second layer and therefore the adsorption enthalpy. This argument explains the slope difference (1/b) for open symbols observed in figure 6.

The fact that the slope corresponding to the formation of the second layer of diHPA is higher indicates a thermodynamically less favored process compared with the adsorption of HSA and the formation of the first monolayer of diHPA on mica. Such energy-based argument can explain the absence of a second layer in the adsorption of PA and HSA on mica, due to the low interaction energy between terminal  $\text{-CH}_3$  groups of the first monolayer and the end groups of the second one ( $\text{-CH}_3$  and  $\text{-COOH}$ ).

## **CONCLUSIONS.**

The adsorption of selected hydroxylated long chain alkyl molecules on mica is used as a model to study the interaction between primary and secondary hydroxyl groups and their influence in the molecular self-assembly process. AFM results have shown that, in addition to the carboxylic group- mica interaction, cohesive forces between alkyl chains arising from hydrogen bonding between secondary hydroxyl groups are proven to be of relevance in the self-assembly of hydroxylated carboxylic acids on mica. Thus, hydrogen bonding contribution extends the adsorption and packing

of 12-hydroxystearic acid beyond the saturation of adsorption sites limit observed for palmitic acid. Secondary hydroxyl groups plays the role of additional anchoring points for alkyl molecules and surface coverage is found to be larger and time dependent for hydroxylated carboxylic acids.

The analysis of AFM images obtained for the adsorption of 12-hydroxystearic and 9(10), 16-dihydroxypalmitic acids on mica reveals a Langmuir type relationship between the surface coverage ( $\theta$ ) and the concentration of the preparation solution ( $c$ ). The adsorption enthalpy derived from the  $1/\theta - 1/c$  plots contains the contribution of both molecule-substrate and molecule-molecule interactions and provides an energy based argument to explain our experimental results.

The combined analysis of molecular interactions in parallel (molecule-substrate) and perpendicular (molecule-molecule) to the alkyl chain axis can explain the growing mode into mono and multilayers observed for the series of hydroxyl acids employed. Thus, as is the case for palmitic and 12-hydroxystearic acids, methyl termination prevents the formation of a second monolayer due to the low energy associated to the  $-\text{CH}_3 \dots \text{HOOC}$ - tail to head interaction. As soon as the methyl end group is replaced by a more reactive hydroxyl termination, the second layer develops, as is the case for the 9(10),16-dihydroxypalmitic acid.

#### **ACKNOWLEDGMENT.**

Support from the Andalusian Regional Government through the 2007 Research Program (Proyecto de Excelencia TEP-02550) is greatly acknowledged.

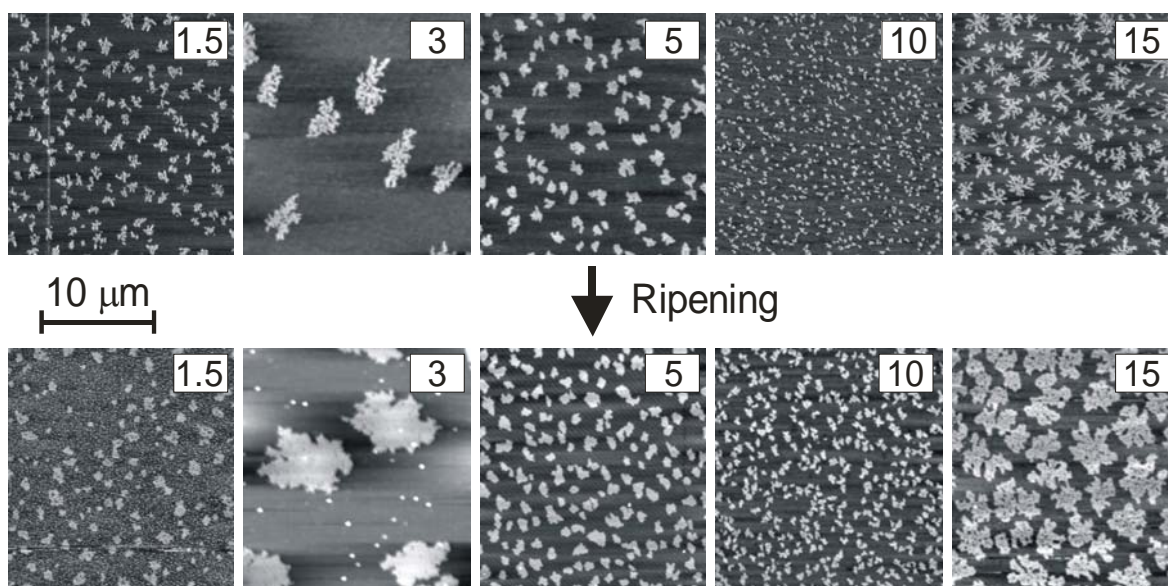


**Figure 1.** Topographic AFM  $20 \times 20 \mu\text{m}^2$  images showing SAMs islands of palmitic acid on mica obtained from chloroform solutions at the concentrations (mM) indicated. The upper row is obtained 24 hours after preparation while lower row is the result of sample ripening for 10-15 days.

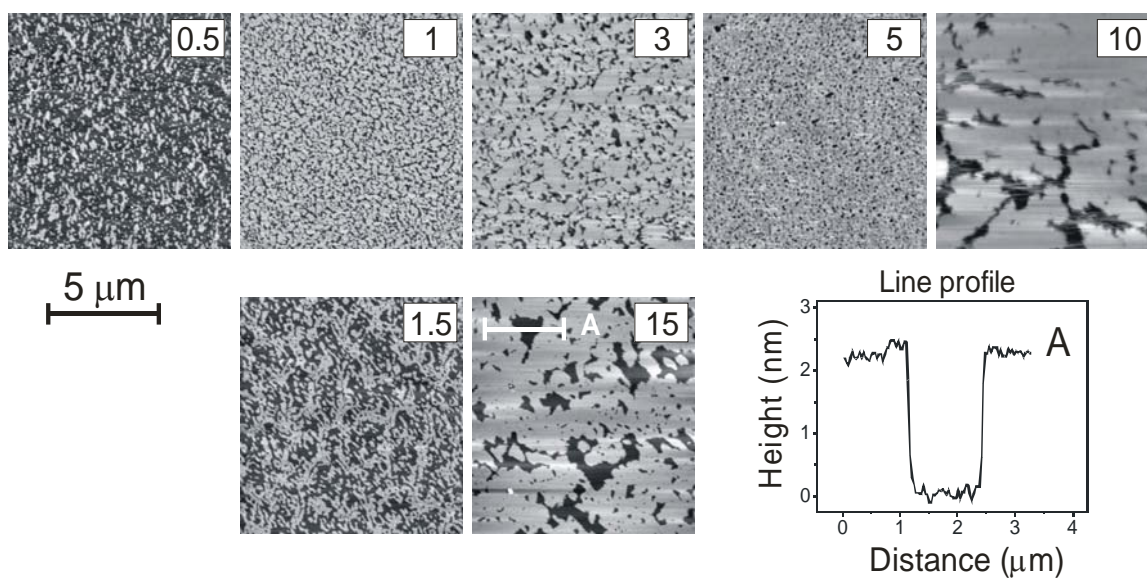


**Figure 2.**  $10 \times 10 \mu\text{m}^2$  AFM images depicting the adsorption and self-assembly of 12-hydroxystearic acid (HSA) on mica from chloroform solutions in the 0.5-15 mM range. HSA adsorption is time dependent as observed by comparing the upper row series (1 minute adsorption time) and two reference images obtained after adsorbing for 30 seconds. In any case, a monolayer is obtained, as shown in the line profile.

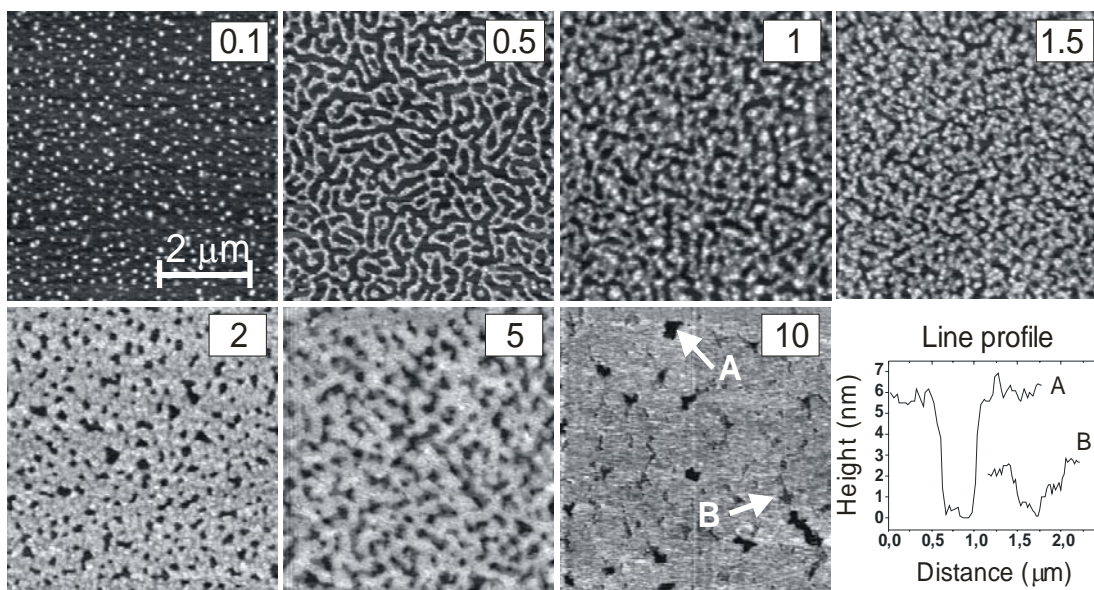


**Figure 3.** Topographic AFM images showing the self-assembly of 9(10), 16 dihydroxypalmitic acid (diHPA) on mica. As the solution concentration is raised, a second monolayer (bright areas) develops.

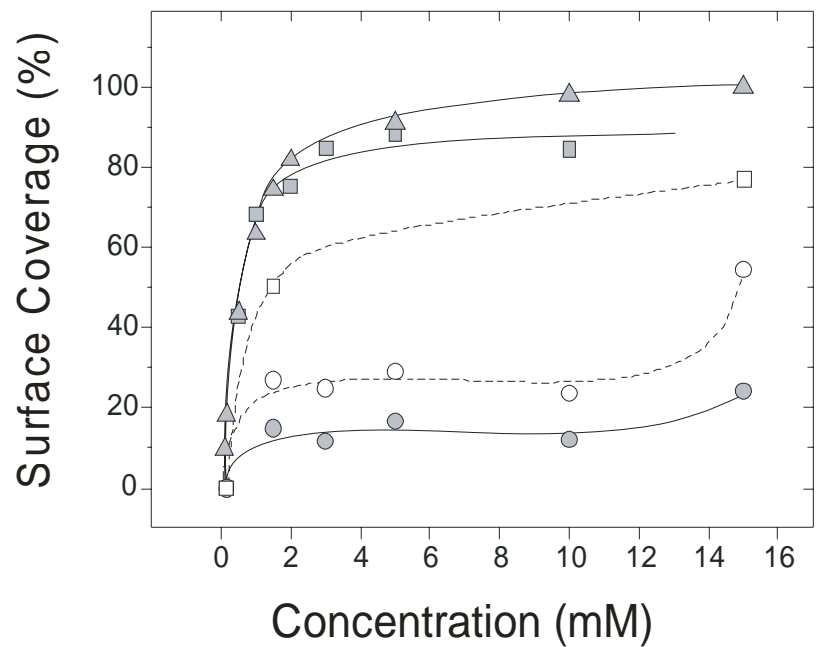


**Figure 4.** Surface coverage evolution vs solution concentration obtained from AFM images for the molecules studied: PA (circles), HSA (squares) and diHPA (triangles). Dashed symbols are the series obtained at typical preparation conditions. Open symbols are for longer ripening PA samples (circles) and shorter adsorption time HSA (squares).



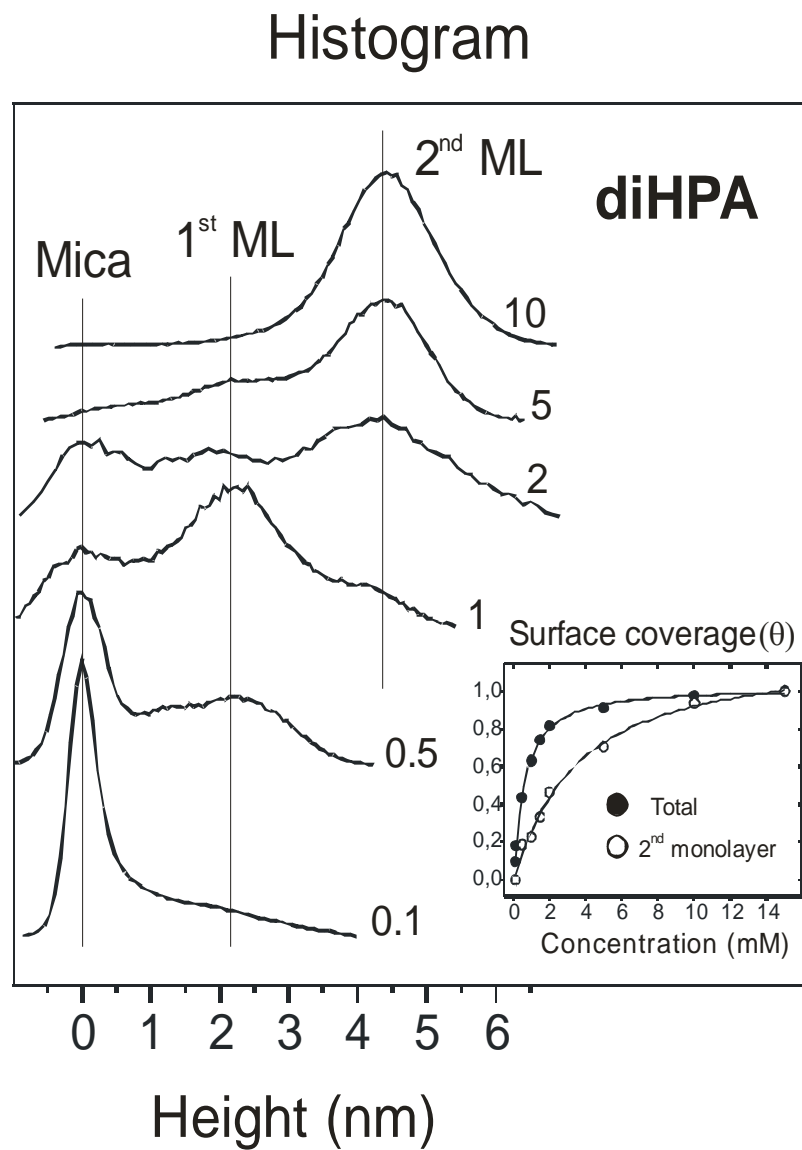


**Figure 5.** Histograms and surface coverage plots showing the second monolayer development in the adsorption and self-assembly of diHPA molecules on mica from increasing concentration solutions.

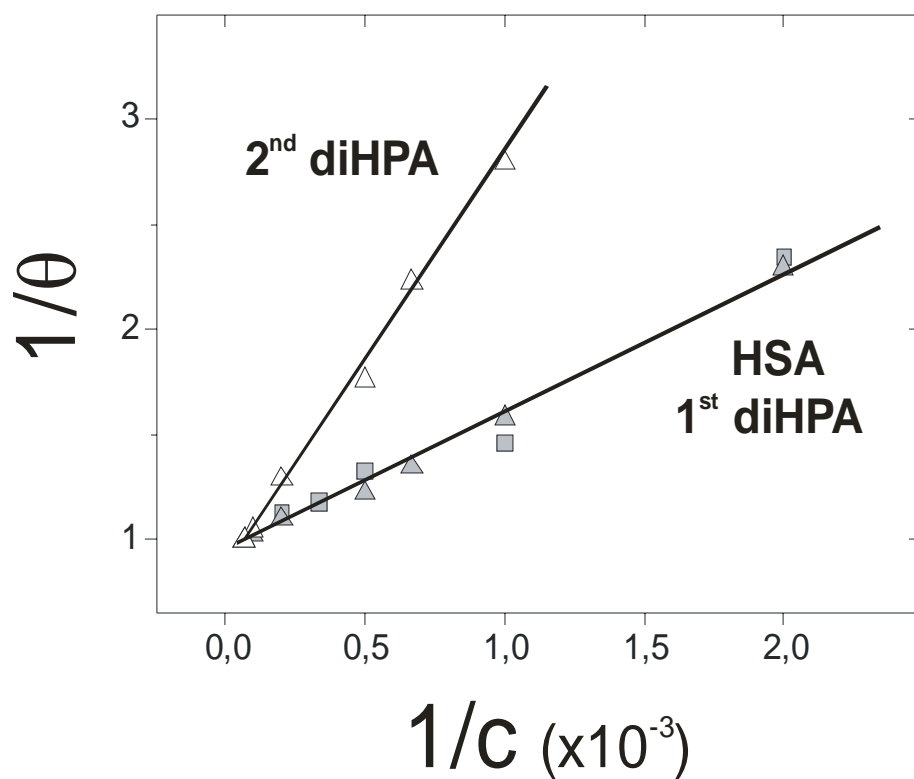


**Figure 6.** Langmuir type isotherms obtained for the adsorption of HSA and diHPA on mica from chloroform solutions. Two set of data are observed: dashed symbols (for HSA (squares) and the first monolayer of diHPA (triangles)) and open symbols (for the second monolayer of diHPA).

## References

---

- <sup>1</sup> Cyr, D. M.; Venkataraman, B.; Flynn, G. W.; Black, A.; Whitesides, G. M. *J. Phys. Chem.* **1996**, *100*, 13747.
- <sup>2</sup> Fang, H.; Giancarlo, L. C.; Flynn, G. W. *J. Phys. Chem. B* **1999**, *103*, 5712.
- <sup>3</sup> Wintgens, D.; Yablon, D. G.; Flynn, G. W. *J. Phys. Chem. B* **2003**, *107*, 173.
- <sup>4</sup> Xu, S. L.; Yin, S. X.; Liang, H. P.; Wang, C.; Wan, L. J.; Bai, C. L. *J. Phys. Chem. B* **2004**, *108*, 620.
- <sup>5</sup> Walton, T. J. *Methods Plant Biochem.* **1990**, *4*, 105.
- <sup>6</sup> Kolattukudy, P. E. *Plant Cuticles: An Integrated Functional Approach*, Kerstiens, G., Ed. BIOS Scientific Publishers: London, **1996**, pp. 83-108.
- <sup>7</sup> Benítez, J. J.; García-Segura, R.; Heredia, A. *Biochimica et Biophysica Acta* **2004**, *1674*, 1.
- <sup>8</sup> Deas, A. H. B.; Holloway, P. J. *Lipids and Lipid Polymers in Higher Plants*, Tevini, M.; Litchenthaler, H. K., Eds. Springer-Verlag: Berlin, **1977**, pp. 293-299.
- <sup>9</sup> Pollard, M.; Beisson, F.; Yonghua, L.; Ohlrogge, J. B. *Trend Plant Sci.* **2008**, *13* (5), 236.
- <sup>10</sup> Heredia-Guerrero, J. A.; Benítez, J. J.; Heredia, A. *BioEssays* **2008**, *30* (3), 273.
- <sup>11</sup> Benítez, J. J.; Heredia-Guerrero, J. A.; Heredia, A. *J. Phys. Chem. C* **2007**, *111*, 9465.
- <sup>12</sup> Deas, A. H. B.; Holloway, P. J. *Lipids and Lipid Polymers in Higher Plants*, Tevini, M.; Litchenthaler, H. K., Eds. Springer-Verlag: Berlin, **1977**, pp. 33-44.
- <sup>13</sup> Stark, R. E.; Yan, B.; Ray, A. K.; Chen, Z.; Fang, X.; Garbow, J. R. *Solid State NMR* **2000**, *16*, 37.
- <sup>14</sup> Garbow, J. R.; Stark, R. E. *Macromolecules* **1990**, *23*, 2814.
- <sup>15</sup> Free software available at [www.nanotec.es](http://www.nanotec.es)
- <sup>16</sup> Benítez, J. J.; Kopta, S.; Ogletree, D. F.; Salmeron, M. *Langmuir* **2002**, *18*, 6096.
- <sup>17</sup> Sikes, H. D.; Woodward, J. T.; Schwartz, D. K. *J. Phys. Chem.* **1996**, *100*, 9093.
- <sup>18</sup> Sikes, H. D.; Schwartz, D. K. *Langmuir* **1997**, *13*, 4704.
- <sup>19</sup> Allara, D. L.; Nuzzo, R. G. *Langmuir* **1985**, *1*, 45.
- <sup>20</sup> Chen, S. H.; Frank, C. W. *Langmuir* **1989**, *5*, 978.
- <sup>21</sup> Teer, E.; Knobler, C. M. *J. Phys. Chem. B* **2000**, *104*, 10053.
- <sup>22</sup> Brzozowska, I.; Figaszewski, Z. A. *Colloid Surface B* **2003**, *30*, 187.
- <sup>23</sup> Benítez, J. J.; Salmeron, M. *J. Chem. Phys.* **2006**, *125*, 044708.